Characterization of cooperative bicarbonate uptake into chloroplast stroma in the green alga *Chlamydomonas reinhardtii*

Takashi Yamano, Emi Sato, Hiro Iguchi, Yuri Fukuda, and Hideya Fukuzawa[1]

Graduate School of Biostudies, Kyoto University, Kyoto 606-8502, Japan

The supply of inorganic carbon (Ci; CO_2 and HCO_3^-) is an environmental rate-limiting factor in aquatic photosynthetic organisms. To overcome the difficulty in acquiring Ci in limiting-CO_2 conditions, an active Ci uptake system called the CO_2-concentrating mechanism (CCM) is induced to increase CO_2 concentrations in the chloroplast stroma. An ATP-binding cassette transporter, HLA3, and a formate/nitrite transporter homolog, LCIA, are reported to be associated with HCO_3^- uptake [Wang and Spalding (2014) *Plant Physiol* 166(4): 2040–2050]. However, direct evidence of the route of HCO_3^- uptake from the outside of cells to the chloroplast stroma remains elusive owing to a lack of information on HLA3 localization and comparative analyses of the contribution of HLA3 and LCIA to the CCM. In this study, we revealed that HLA3 and LCIA are localized to the plasma membrane and chloroplast envelope, respectively. Insertion mutants of *HLA3* and/or *LCIA* showed decreased Ci affinities/accumulation, especially in alkaline conditions where HCO_3^- is the predominant form of Ci. HLA3 and LCIA formed protein complexes independently, and the absence of LCIA decreased *HLA3* mRNA accumulation, suggesting the presence of unidentified retrograde signals from the chloroplast to the nucleus to maintain *HLA3* mRNA expression. Furthermore, although single overexpression of HLA3 or LCIA in high CO_2 conditions did not affect Ci affinity, simultaneous overexpression of HLA3 with LCIA significantly increased Ci affinity/accumulation. These results highlight the HLA3/LCIA-driven cooperative uptake of HCO_3^- and a key role of LCIA in the maintenance of HLA3 stability as well as Ci affinity/accumulation in the CCM.

bicarbonate uptake | *Chlamydomonas* | chloroplast envelope | CO_2-concentrating mechanism | photosynthesis

Inorganic carbon (Ci; CO_2 and HCO_3^-) transport is essential for a wide range of biological processes such as CO_2 metabolism, cellular pH homeostasis, and photosynthesis. Because HCO_3^- is not freely permeable to biological membranes, it must be transported across membranes by HCO_3^- transporters or channels. HCO_3^- transporters have been studied extensively in mammals and been found to cluster into solute carrier (SLC) 4 and SLC 26 families (1). In cyanobacteria, five types of Ci transporters have been identified (2), including three HCO_3^- transporters and two NAD(P)H dehydrogenase-dependent CO_2 uptake systems. In land plants, aquaporin-mediated CO_2 permeation has been suggested to play physiological roles in photosynthesis (3), and in a marine diatom, SLC4 family protein localized to the plasma membrane (PM) facilitates HCO_3^- uptake (4). However, no studies have validated the entire route of HCO_3^- transport from the outside of cells to the chloroplast stroma through the PM and chloroplast envelope (CE) in photosynthetic organisms.

Aquatic conditions are not well suited for efficient photosynthesis because the CO_2 diffusion rate is ~10,000-fold lower compared with that in atmospheric conditions (5). Therefore, aquatic photosynthetic organisms, including microalgae, are frequently exposed to limiting CO_2 stress. To acclimate to this stress, most microalgae possess a CO_2-concentrating mechanism (CCM) to accumulate CO_2 around the CO_2 fixation enzyme ribulose 1,

5-bisphosphate carboxylase/oxygenase (Rubisco) and to maintain adequate photosynthetic efficiency (6, 7).

The green alga *Chlamydomonas reinhardtii* has been used as a model organism for molecular and physiological studies of the CCM since it was first identified (8). A model of the CCM has been proposed based on the subcellular structure of *C. reinhardtii* (9, 10). Environmental Ci is transported to the chloroplast stroma by Ci transporters localized to the PM and CE. Carbonic anhydrase (CA) localized to the chloroplast stroma is predicted to contribute to the maintenance of the Ci pool, in the form of HCO_3^-, by rapid conversion of CO_2 to HCO_3^-, thereby preventing the loss of CO_2 by diffusion (11). It is known that tubule-like thylakoid membranes penetrate into the pyrenoid (12), a Rubisco-enriched structure in the chloroplast. HCO_3^- in the stroma is transported into the acidic thylakoid lumen by a putative channel or transporter localized to the thylakoid membrane, and HCO_3^- is rapidly converted to CO_2 by a constitutively expressed CA (13, 14). Then, CO_2 diffuses from the thylakoid lumen into the pyrenoid matrix and is fixed by Rubisco. It was also reported that *C. reinhardtii* acclimates to two distinct limiting CO_2 conditions, termed low CO_2 (LC; ~0.03–0.5% CO_2 or 7–70 μM CO_2) and very low CO_2 (VLC; <0.02% CO_2 or <7 μM CO_2) (15, 16), and different types of Ci uptake systems could function in the CCM in these separate conditions (16).

To identify CCM-associated components, several transcriptome analyses have been performed (17–22), and several genes encoding membrane proteins were focused on as candidate Ci transporter genes, including *LCI1* (low CO_2 inducible gene 1) (23),

Significance

The entry of inorganic carbon (Ci; CO_2 and HCO_3^-) into cells involves many biological processes in both animals and plants, and aquaporins as well as bicarbonate transporters play roles in Ci transport. Although transporting external HCO_3^- into the stroma through the chloroplast envelope is one of the rate-limiting factors for aquatic photosynthetic organisms, specific molecular components in this process have not yet been identified experimentally. Molecular identification of proteins essential for Ci uptake located in the chloroplast envelope and in the plasma membrane documented in this study helps in understanding how aquatic photosynthetic organisms developed machinery to acclimate to CO_2-limiting environment and to maintain adequate levels of photosynthesis for survival or growth.

PLANT BIOLOGY

LCIA (low CO_2 inducible gene A) (19), and *HLA3* (high light activated 3) (24).

LCI1 is localized to the PM (25), and its expression is regulated by the MYB-transcription factor LCR1 (low CO_2 stress response 1) (26). When *LCI1* was artificially expressed in HC conditions, the cells showed increases in the internal Ci pool, suggesting that LCI1 is directly or indirectly associated with Ci uptake (25). LCIA (also known as NAR1.2) is a homolog of the nitrate transporter NAR1 and belongs to the formate/nitrite transporter family (27). Although the expression of other *NAR1* family genes of *C. reinhardtii* is mainly regulated by nitrogen source, *LCIA* is specifically induced in LC conditions and is not under the control of nitrogen source (19). LCIA was predicted to localize to the CE (19), and this prediction was supported by indirect immunofluorescence assay evidence (16). Functional expression analysis using *Xenopus* oocytes showed transport activity of LCIA for both HCO_3^- and NO_2^- (27), and LCIA appears to be associated with HCO_3^- uptake in VLC conditions from analysis of an insertion mutant (16). HLA3 is an ATP-binding cassette (ABC) transporter of the multidrug resistance-related protein subfamily, and its transcription is induced by high light and LC conditions (19, 24). Although HLA3 is predicted to localize to the PM (10), no experimental data are available at present. Knockdown (KD) of *HLA3* mRNA expression resulted in modest decreases in photosynthesis affinity, but simultaneous KD of *LCIA* and *HLA3* mRNAs caused a dramatic decrease in growth rate, Ci uptake activity, and photosynthetic Ci affinity, especially in alkaline conditions, where HCO_3^- is the predominant form of Ci (28).

In this study, by use of indirect immunofluorescence assays and membrane fractionation, the subcellular localization of HLA3 was elucidated. In addition, by analyses of the photosynthetic characteristics of *HLA3* and *LCIA* single insertion mutants, an *HLA3*/*LCIA* double insertion mutant, and overexpressing strains of *HLA3* and/or *LCIA*, we concluded that HLA3 and LCIA are cooperatively associated with HCO_3^- uptake across the PM and CE, respectively.

Results

Accumulation of HLA3 and LCIA in Very Low CO_2 Conditions. First, to define the acclimated states of limiting CO_2 conditions (LC or VLC) of cells grown in liquid culture, total Ci concentration in the culture medium at pH 7.0 was measured, and consequent CO_2 concentrations were calculated (Fig. 1*A*). CO_2 concentrations supplied with 0.04% CO_2 for 1, 2, 4, 6, and 12 h were estimated as 6.3, 3.1, 2.9, 1.9, and 1.8 μM, respectively, which correspond to the range for VLC (<7 μM CO_2) (16). Thus, we defined the limiting CO_2 conditions of liquid culture as VLC throughout this study. Next, the time course accumulation of HLA3 and LCIA after VLC induction was examined (Fig. 1*A*). The accumulation of these proteins started within 1 h and reached their maximum levels within 4 h, as was the case for LCI1 used as a control of VLC induction. The molecular masses of HLA3 and LCIA were detected at sizes of ~133 and 27 kDa, respectively (Fig. S1*A* and *SI Results and Discussion*).

Subcellular Localization of HLA3 and LCIA. To analyze the subcellular localization of HLA3, an indirect immunofluorescence assay was performed (Fig. 1*B*). Fluorescence signals from an anti-HLA3 antibody were detected peripherally, suggesting the localization of HLA3 to the PM. Fluorescence signals from an anti-LCIA antibody were detected as a single cup-shaped structure (Fig. 1*B*), as in the previous study (16). To further clarify the localization of HLA3 and LCIA biochemically, protein samples from total cell, PM, and CE fractions were probed with antibodies against HLA3, LCI1, H+-ATPase, LCIA, and CCP1 (Fig. 1*C* and *SI Results and Discussion*). LCI1 and H+-ATPase were enriched in the PM fraction, consistent with the PM localization of these
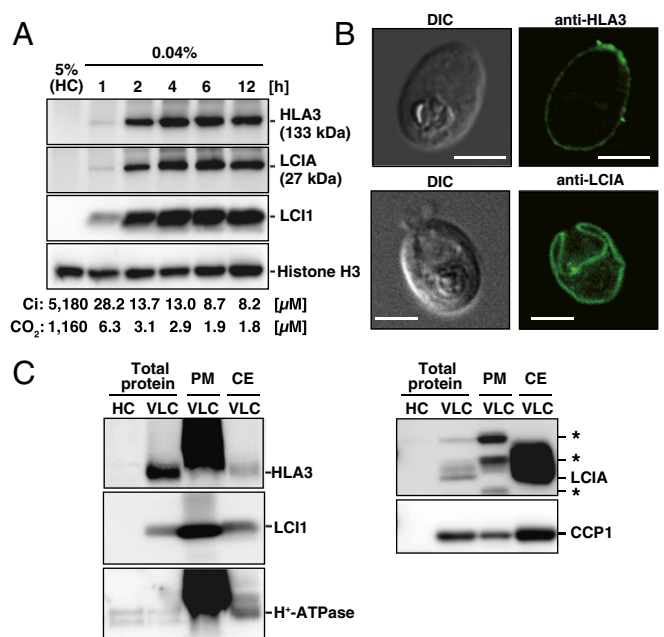

Fig. 1. Accumulation and subcellular localization of HLA3 and LCIA. (*A*) Time-course of accumulation of HLA3, LCIA, and LCI1 proteins in WT cells. For induction of limiting-CO_2 conditions, cells supplied with 5% CO_2 (high CO_2; HC) were centrifuged, suspended in new fresh medium, and cultured with 0.04% CO_2 for 1, 2, 4, 6, and 12 h. Histone H3 was used as a loading control. The total Ci concentrations and calculated CO_2 concentrations after each induction time are also indicated below the figures. Using an HCO_3^-/CO_2 ratio of 4.47 at pH 7.0, CO_2 concentrations were calculated using the equation ($pH = pK_a + \log_{10} [HCO_3^-]/[CO_2]$), where pK_a was an acid dissociation constant of 6.35. (*B*) Subcellular localization of HLA3 and LCIA by an indirect immunofluorescence assay. WT cells were grown in very low CO_2 (VLC) for 12 h. DIC, differential interference contrast. (Scale bars, 5 μm.) (*C*) Immunoblot analysis in isolated plasma membrane (PM) and chloroplast envelope (CE) fractions with antibodies against HLA3, LCI1, H+-ATPase, LCIA, and CCP1. Asterisks indicate nonspecific bands.

proteins (25, 29). Similarly, a notable enrichment of HLA3 was observed in the PM fraction. LCIA was highly enriched in the CE fraction, where CE protein CCP1 (30) was also enriched. From these results, we concluded that HLA3 and LCIA were localized to the PM and CE, respectively.

Isolation of an *HLA3* Insertion Mutant and Photosynthetic Characteristics. To evaluate the degree of contribution of HLA3 to the CCM, we isolated an *HLA3* insertion mutant from our paromomycin resistance gene-tagged mutant library by PCR-based screening, as described previously (31), and designated the strain Hin-1 (Fig. S2 *A–C* and *SI Results and Discussion*).

Next, the photosynthetic characteristics were evaluated by measuring the rates of Ci-dependent O_2 evolution of WT, Hin-1, and the complemented strain Hin-1C grown in VLC at different pH. $K_{0.5}$ (Ci) values, the Ci concentration required for half maximal O_2-evolving activity, of WT and Hin-1 were similar at pH 6.2 (ratio of HCO_3^-:CO_2 = 0.7:1) and pH 7.8 (HCO_3^-:CO_2 = 28:1), indicating that the difference in photosynthetic Ci affinity between WT and Hin-1 was not significant (Fig. 2*A*). Because *HLA3* KD strains showed retarded growth rates at pH 9.0 (28) where the ratio of HCO_3^-:CO_2 = 446:1 and HCO_3^- was the predominant form of Ci, we evaluated the changes in Ci affinity during acclimation to VLC at pH 9.0 in a time course analysis (Fig. 2*B*). Both WT and Hin-1 showed a gradual decrease in $K_{0.5}$ (Ci) during acclimation to VLC. However, although WT in VLC at 6 h showed almost the same Ci affinity compared with that at 12 h (241 ± 87 μM at 6 h and 290 ± 50 μM at 12 h), Hin-1 still showed much
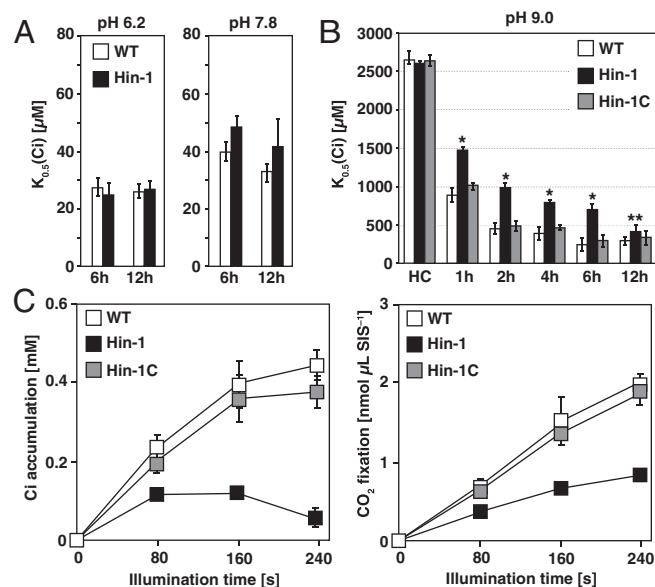
Fig. 2. Characterization of an *HLA3* insertion mutant. (*A*) Inorganic carbon (Ci) affinity of WT and *HLA3* insertion mutant (Hin-1) grown in very low CO_2 (VLC) for 6 or 12 h. Photosynthetic O_2-evolving activity was measured with different external Ci concentrations at pH 6.2 or 7.8, and the respective $K_{0.5}$ (Ci) values, the Ci concentration required for half maximum O_2-evolving activity, were calculated. (*B*) Ci affinity of WT, Hin-1, and complemented Hin-1 (Hin-1C) grown in high CO_2 (HC) or VLC for 1, 2, 4, 6, and 12 h. O_2-evolving activity was measured at pH 9.0. *$P < 0.01$ and **$P < 0.05$ by Student *t* test. (*C*) Accumulation and fixation of Ci in WT, Hin-1, and Hin-1C. Cells were grown in VLC for 6 h, and intracellular Ci accumulation (*Left*) and CO_2 fixation (*Right*) at pH 9.0 were measured using a silicone oil layer method. SIS, sorbitol impermeable space.

lower Ci affinity especially at 6 h (691 ± 143 μM at 6 h and 405 ± 57 μM at 12 h), and the decreased Ci affinity was restored in Hin-1C (296 ± 78 μM at 6 h and 333 ± 89 μM at 12 h). These results suggested that other Ci uptake systems could compensate for the absence of HLA3 and contribute to the increase in Ci affinity at 12 h and that measuring photosynthetic characteristics at 6 h was appropriate for evaluating the contribution of HLA3 to the CCM.

To evaluate the contribution of HLA3 to actual Ci uptake activity, the accumulation and fixation of [^{14}C]-labeled Ci in WT, Hin-1, and Hin-1C grown in VLC for 6 h were measured (Fig. 2*C*). Hin-1 showed significantly lower levels of Ci accumulation of 0.12 mM (0.57-fold of Hin-1C), 0.12 mM (0.32-fold), and 0.06 mM (0.17-fold) after 80, 160, and 240 s of illumination, respectively, and CO_2 fixation of 0.37 nmol·μL SIS^{-1} (0.59-fold), 0.67 nmol·μL SIS^{-1} (0.49-fold), and 0.83 nmol·μL SIS^{-1} (0.44-fold), respectively, compared with that of Hin-1C. These results indicated that HLA3 has a meaningful role in HCO_3^- uptake in VLC conditions.

Isolation of *LCIA* Insertion Mutants and Photosynthetic Characteristics. A disruption mutant of *LCIA* has been characterized, and the contribution of LCIA to the CCM has been reported (16). To compare the degrees of the contributions of HLA3 and LCIA to the CCM, we also isolated two *LCIA* insertion mutants (Fig. S2 *D–G* and *SI Results and Discussion*), designated as Ain (Ain-1 and Ain-2), and compared the photosynthetic characteristics with Hin-1. Interestingly, accumulation of HLA3 was much lower in Ain compared with that in WT, and this decreased accumulation of HLA3 was restored in the complemented strains Ain-1C and Ain-2C (Fig. 3*A*). This result was in sharp contrast to that of LCI1 and LCIB (32), which were not affected by the impairment of the *LCIA* (Fig. 3*A*).

Next, the photosynthetic characteristics of Ain-1, Ain-2, Ain-1C, and Ain-2C were evaluated. As in the case of Hin-1, the $K_{0.5}$ (Ci) of Ain-1 and Ain-2 was similar to WT at pH 6.2 (Fig. 3*B*). However, in contrast to Hin-1, the $K_{0.5}$ (Ci) of Ain-1 (57 ± 2 μM at 6 h and 56 ± 3 μM at 12 h) and Ain-2 (57 ± 1 μM at 6 h and 57 ± 2 μM at 12 h) was significantly higher than that of WT (40 ± 3 μM at 6 h and 33 ± 3 μM at 12 h), Ain-1C (38 ± 2 μM at 6 h and
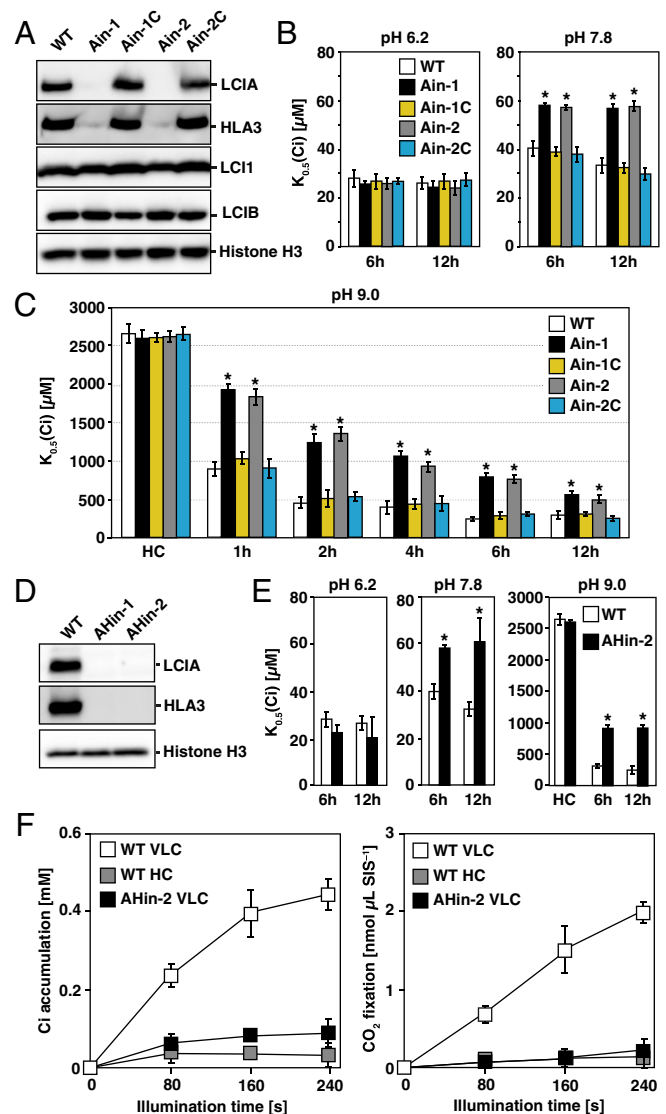

Fig. 3. Characterization of *LCIA* insertion mutants and an *LCIA/HLA3* double-insertion mutant. (*A*) Accumulation of LCIA, HLA3, LCI1, and LCIB in WT, *LCIA* insertion mutants (Ain-1 and Ain-2), and their complemented strains (Ain-1C and Ain-2C). Cells were grown in very low CO_2 (VLC) for 12 h. (*B*) Inorganic carbon (Ci) affinity of WT, Ain-1, Ain-2, Ain-1C, and Ain-2C grown in VLC for 6 or 12 h. Photosynthetic O_2-evolving activity was measured with different external Ci concentrations at pH 6.2 or 7.8, and the respective $K_{0.5}$ (Ci) values, the Ci concentration required for half maximum O_2-evolving activity, were calculated. *$P < 0.01$. (*C*) Ci affinity of WT, Ain-1, Ain-2, Ain-1C, and Ain-2C grown in high CO_2 (HC) or VLC for 1, 2, 4, 6, and 12 h. O_2-evolving activity was measured at pH 9.0. *$P < 0.01$. (*D*) Accumulation of HLA3 and LCIA in WT and *LCIA/HLA3* double-insertion mutants (AHin-1 and AHin-2) grown in VLC for 12 h. (*E*) Ci affinity of WT and AHin-2 grown in HC or VLC for 6 or 12 h. O_2-evolving activity was measured at pH 6.2, 7.8, or 9.0. *$P < 0.01$. (*F*) Accumulation and fixation of Ci in WT and AHin-2. Cells were grown in HC or VLC for 6 h, and intracellular Ci accumulation (*Left*) and CO_2 fixation (*Right*) were measured at pH 9.0. SIS, sorbitol impermeable space.

32 ± 2 μM at 12 h), and Ain-2C (37 ± 3 μM at 6 h and 29 ± 2 μM at 12 h), even at pH 7.8 (Fig. 3B). At pH 9.0, although Ain also showed gradual decreases in $K_{0.5}$ (Ci) during acclimation to VLC, these cells always showed lower Ci affinity than Hin-1 (Fig. 2B), as well as WT and complemented strains (Fig. 3C). These results suggested a significant contribution of LCIA to increases in Ci affinity and to maintaining HLA3 stability in the CCM.

Isolation of *LCIA/HLA3* Double-Insertion Mutants and Photosynthetic Characteristics. Because Ci affinity in VLC at 12 h was higher than that at 6 h in both *HLA3* and *LCIA* single mutants, either protein could partially complement each other to increase Ci affinity. Thus, we expected that *LCIA/HLA3* double-insertion mutants would show an additive decrease in Ci affinity compared with the single-insertion mutants. Thus, we isolated double-insertion mutants by crossing one of the Ain-2 progeny with Hin-1 and designated these as AHin (AHin-1 and AHin-2; Fig. 3D, Fig. S2 H–K, and *SI Results and Discussion*).

Next, the photosynthetic characteristics of AHin-2 were evaluated (Fig. 3E). As in the case of Hin-1 and Ain, the $K_{0.5}$ (Ci) of AHin-2 was similar to WT at pH 6.2. At pH 7.8, the $K_{0.5}$ (Ci) of AHin-2 (58 ± 2 μM at 6 h and 61 ± 10 μM at 12 h) was significantly higher than that of WT, but it was similar to Ain. At pH 9.0, AHin-2 showed lower Ci affinity than both Hin-1 and Ain, and Ci affinity was not increased even at 12 h (898 ± 78 μM at 6 h and 901 ± 94 μM at 12 h). Ci accumulation and fixation in AHin-2 grown in VLC at 6 h was also measured (Fig. 3F). After 80, 160, and 240 s of illumination, AHin-2 showed substantially decreased Ci accumulation of 0.05 mM (0.21-fold of WT and 0.41-fold of Hin-1), 0.06 mM (0.16-fold and 0.53-fold), and 0.06 mM (0.15-fold and 1.0-fold), respectively, and CO_2 fixation of 0.07 nmol·μL SIS^{-1} (0.1-fold and 0.2-fold), 0.12 nmol·μL SIS^{-1} (0.08-fold and 0.17-fold), and 0.14 nmol·μL SIS^{-1} (0.07-fold and 0.17-fold), respectively, compared with that of WT and Hin-1.

Finally, the effect of absence of LCIA and/or HLA3 on cell growth was examined. Growth rates were measured in VLC at pH 8.4 (Fig. S2L) because there were no significant differences at pH 7.8, and none of the cell lines could grow at pH 9.0. The doubling time of WT was 7.2 h and that of Hin-1, Ain-1, Ain-2, and AHin-2 increased significantly to 7.6, 9.5, 9.3, and 12.7 h, respectively, reflecting the degree of decreased Ci affinity of each cell line. These results highlighted an additive decrease in Ci affinity/accumulation/growth rates of the double-insertion mutant compared with the *HLA3* or *LCIA* single-insertion mutants.

Isolation of LCIA and/or HLA3 Overexpressing Strains and Photosynthetic Characteristics. To demonstrate the physiological function of LCIA and HLA3 more directly, the photosynthetic characteristics of cells overexpressing LCIA and/or HLA3 were examined in HC conditions where other VLC-inducible proteins were not induced. For overexpression, two chimeric plasmids, pTY2b-LCIA and pTY2b-HLA3, were constructed (Fig. S3A). These plasmids allowed the induction of *LCIA* and *HLA3* transcripts by switching the nitrogen source from NH_4^+ to NO_3^- irrespective of the CO_2 conditions. In this study, we cultured the cells with four combinations of nitrogen sources in the medium and CO_2 concentrations, designated as HC-NH_4^+, HC-NO_3^-, VLC-NH_4^+, and VLC-NO_3^-.

First, we transformed WT cells with pTY2b-LCIA or pTY2b-HLA3 separately. The transformants showed accumulation of LCIA or HLA3 when grown in HC-NO_3^- conditions and were designated as Aox (Aox-1 and Aox-2) and Hox (Hox-1 and Hox-2), respectively (Fig. S3 B and C and *SI Results and Discussion*). Next, by introducing pTY2b-HLA3 into Aox-1, we generated two independent transformants expressing LCIA and HLA3 simultaneously and designated these as AHox (AHox-1 and AHox-2; Fig. S3D). Accumulation of HLA3 in AHox-1 and AHox-2 was the same as that of VLC-grown WT. To isolate a strain overexpressing

both LCIA and HLA3 with greater abundance, the progeny of Aox-1 was crossed with Hox-1 and a strain designated as AHox-3 was obtained (Fig. S3E).

Next, to evaluate the effect of LCIA and/or HLA3 overexpression on the photosynthetic characteristics, rates of O_2 evoluton at pH 6.2, 7.8, and 9.0 and Ci accumulation at pH 9.0 of these strains were measured. In Aox, there were no differences in Ci affinity at pH 7.8 and pH 9.0, as well as Ci accumulation compared with WT (Fig. 4A and Table S1–S3). In contrast, HC-NO_3^--grown Hox showed a small but significant increase of Ci accumulation of 0.08 mM (2.5-fold of WT at 80 s), 0.07 mM (1.5-fold at 160 s), and 0.13 mM (2.4-fold at 240 s) in Hox-2, compared with that of HC-NO_3^--grown WT, but the phenotype led to a slight increase in Ci affinity only at pH 9.0 in Hox-2 (Fig. 4B), suggesting that Ci in the cytosol transported by HLA3 could not efficiently enter the chloroplast stroma in the absence of LCIA. On the other hand, Ci affinity at pH 6.2 was increased in
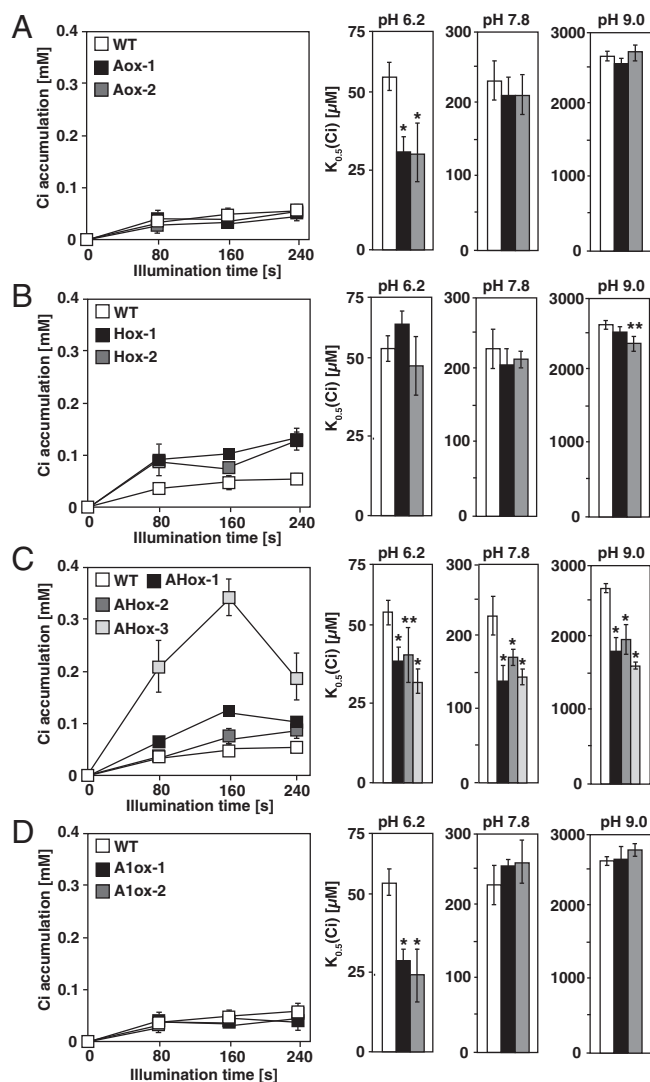

Fig. 4. Characterization of LCIA- and HLA3-overexpressing strains. Accumulation of inorganic carbon (Ci) (*Left*) and Ci affinity (*Right*) in WT and in strains overexpressing LCIA (A), HLA3 (B), LCIA/HLA3 (C), and LCIA/LCI1 (D). Cells were grown in high CO_2-NO_3^- for 12 h, and Ci accumulation was measured at pH 9.0. For Ci affinity, O_2-evolving activity was measured with different external Ci concentrations at pH 6.2, 7.8, or 9.0 and the respective $K_{0.5}$ (Ci) values, the Ci concentration required for half maximum O_2-evolving activity, were calculated. *$P < 0.01$ and **$P < 0.05$.

LCIA-overexpressing Aox (Fig. 4A) and AHox (Fig. 4C), but not in Hox (Fig. 4B).

In contrast to Aox and Hox, AHox showed a significant increase in Ci affinity and Ci accumulation compared with WT at alkaline conditions (Fig. 4C and Tables S2 and S3). In particular, HC-NO$_3^-$-grown AHox-3 showed substantially increased Ci accumulation of 0.21 mM (6.3-fold of WT at 80 s), 0.34 mM (6.8-fold at 160 s), and 0.19 mM (3.6-fold at 240 s) compared with that of HC-NO$_3^-$-grown WT. Consequently, the respective $K_{0.5}$ (Ci) of AHox-1, AHox-2, and AHox-3 decreased to 141 ± 20 (0.61-fold of WT) at pH 7.8 and to 1,821 ± 201 (0.68-fold of WT), 1,980 ± 198 (0.75-fold), and 1,626 ± 49 μM (0.61-fold) at pH 9.0. In HC-NH$_4^+$ conditions at pH 7.8 where *LCIA* and *HLA3* were not induced, the respective $K_{0.5}$ (Ci) of 257 ± 28, 250 ± 30, and 262 ± 29 μM in AHox-1, AHox-2, and AHox-3 was not significantly different from that of 273 ± 31 μM in WT (Table S2). These results indicated that NO$_3^-$-induced overexpression of LCIA and HLA3 could enhance HCO$_3^-$ accumulation in the chloroplast stroma and increase Ci affinity.

Although PM-localized LCI1 could be associated with Ci uptake (25), the preferred Ci species of LCI1 remained elusive. To evaluate the degree of LCIA/HLA3-driven HCO$_3^-$ uptake activity, we also isolated six transformants expressing LCIA with LCI1 by introducing pTY2b-LCI1 (Fig. S3A) into Aox-1 and designated two representatives as A1ox (A1ox-1 and A1ox-2; Fig. S3F). There were no differences in Ci accumulation and affinity in alkaline conditions compared with WT (Fig. 4D and Table S2 and S3), suggesting that LCI1 was not related to direct HCO$_3^-$ uptake along with LCIA.

A Defect in LCIA Led to a Decrease in HLA3 Accumulation Caused by Suppression of *HLA3* mRNA Accumulation. As described above, accumulation of HLA3 was much lower in Ain compared with that in WT (Fig. 3A). This result suggested two possibilities. First, HLA3 and LCIA undergo a physical interaction where the PM is associated with the CE and the absence of LCIA causes instability of HLA3. Second, the absence of LCIA causes the repression of *HLA3* mRNA accumulation.

To examine the former possibility, the molecular masses of LCIA and HLA3 in vivo were estimated by Blue Native-PAGE. We expected that LCIA and HLA3 should be detected with the same molecular mass in nondenaturing conditions if these two proteins interact and form a complex. However, using 1.0% n-dodecyl β-D-maltoside (DDM) as a detergent, LCIA and HLA3 were detected with different sizes of ~240 and 580 kDa, respectively (Fig. 5A). We also estimated the molecular masses using different DDM concentrations (0.25%, 0.5%, 1.0%, or 2.0%) or using formaldehyde cross-linker, and LCIA and HLA3 were still detected at 240 and 580 kDa, respectively (Fig. S4 A and B). Furthermore, LCIA and HLA3 could form respective complexes with the same molecular masses even in Aox, Hox, and AHox cells grown in HC-NO$_3^-$ conditions (Fig. S4C). These results strongly suggested that LCIA and HLA3 did not interact physically in vivo and at least VLC-inducible proteins other than LCIA and HLA3 were not associated with the formation of the respective protein complexes.

For the latter possibility, *HLA3* mRNA accumulation was evaluated by quantitative real-time PCR (Fig. 5B). The sequences of primers used are listed in Table S4. *HLA3* mRNA levels were significantly reduced in Ain-1 and Ain-2 grown in VLC, but mRNA accumulation was restored in the complemented strains. In contrast, the mRNA levels of *LCIA* were not affected in Hin-1 (Fig. 5B), and those of other VLC-inducible genes *LCIB* and *LCI1* were also largely unchanged in Ain-1 and Ain-2, as well as Hin-1 (Fig. S4D). These results suggested that LCIA localized to the CE could affect the mRNA
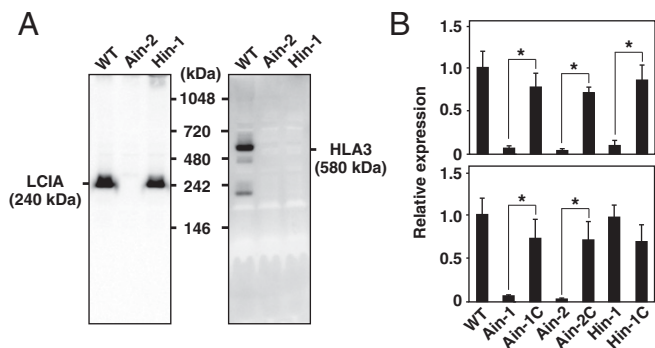

Fig. 5. Molecular masses of LCIA and HLA3 in nondenaturing conditions and effect of the absence of LCIA on *HLA3* mRNA accumulation. (A) Molecular masses of LCIA and HLA3 in nondenaturing conditions. Total proteins were solubilized using 1.0% n-dodecyl β-D-maltoside and separated by blue-native PAGE. (B) Quantitative real-time PCR analyses of *HLA3* (*Upper*) and *LCIA* (*Lower*) in WT, Ain-1, Ain-2, Ain-1C, Ain-2C, Hin-1, and Hin-1C. These cells were grown in very low CO$_2$ conditions for 4 h. Expression of each gene was normalized to *CBLP*. Data in all experiments indicate mean value ± SD from three biological replicates. *P < 0.01.

expression level of *HLA3* and subsequently caused a decrease in HLA3 protein accumulation.

Discussion

In this study, by characterizing the photosynthetic phenotype of *LCIA* and *HLA3* insertion/overexpressing strains, it was revealed that HLA3 and LCIA are parts of the mechanism of HCO$_3^-$ uptake through the PM and CE. These results elucidated a route of HCO$_3^-$ uptake from the outside of cells to the chloroplast stroma by the cooperative function of HLA3 and LCIA.

Although LCIA could be associated with HCO$_3^-$ uptake, the molecular mechanism remains elusive. LCIA is a homolog of formate transporter FocA and contains five amino acid residues (Fig. S2F) corresponding to those shown to form the pore of FocA (19, 33). FocA forms a symmetric pentamer that closely resembles the structure of aquaporin (33) and facilitates formate transport as a channel. Considering that LCIA was detected at 240 kDa in nondenaturing conditions (Fig. 5A), LCIA forms a protein complex as in the case of FocA. Furthermore, considering that the capacity for formate passage by FocA is increased by mutations of the aforementioned amino acids to smaller residues (33), examining the effect of similar mutations in LCIA could be helpful in elucidating the function of LCIA as a potential HCO$_3^-$ channel. Relating to this hypothesis, a significant increase in Ci affinity at pH 6.2 was observed in LCIA-overexpressing strains (Fig. 4 A, C, and D). Considering that external CO$_2$ at pH 6.2 should enter the cytoplasm continuously by passive influx, LCIA could function as a channel and cause an increase in the apparent Ci conductance with a minimal concentration gradient without waiting for a notable increase in Ci accumulation in the cytoplasm. In contrast, endogenous levels of HLA3 in HC conditions were not sufficient for Ci permeation toward the chloroplast stroma even with increased cytosolic Ci accumulation (Fig. 4B). These results suggested the functional importance of LCIA as a bottle neck step for increases in photosynthetic conductance across the CE.

By measuring the Ci accumulation and affinity of LCIA/LCI1-overexpressing strains and comparing the results with those of LCIA/HLA3-overexpressing strains, the degree of LCIA/HLA3-dirven HCO$_3^-$ uptake activity was evaluated (Fig. 4D). However, there were no differences in Ci accumulation and affinity at pH 9.0 compared with WT, suggesting that LCI1 was not related to the direct HCO$_3^-$ uptake along with LCIA. Furthermore, although it was reported that Ci affinity was increased by the single overexpression of LCI1 at pH 7.8 (25), A1ox did not show a

significant increase in Ci affinity in the same pH conditions. This discrepancy could be caused by the difference in $K_{0.5}$ (Ci) values of the strains examined. For overexpressing LCI1 in the previous report, strain lcr1 deficient in mRNA expression for at least three genes, *LCI1*, *CAH1*, and *LCI6* (26), was used, and its $K_{0.5}$ (Ci) was 445 ± 38 μM in HC conditions at pH 7.8 (25). In contrast, the $K_{0.5}$ (Ci) of strain C9 used as WT in this study was 230 ± 27 μM in the same conditions, which was almost the same as 245 ± 38 μM when LCI1 was overexpressed in *lcr1* (25). Thus, the effect of overexpressing LCI1 could be masked in A1ox cells.

By means of *LCIA* insertion mutant analyses, it was shown that LCIA localized to the CE affected *HLA3* mRNA expression in the nucleus (Fig. 5B), which could throw new light on understanding the regulation of *LCIA* and *HLA3*. Considering that *LCIA* expression was not affected by the absence of HLA3 (Fig. 5B), there may be unidentified retrograde signals from the chloroplast to the nucleus for maintaining *HLA3* mRNA expression. This possibility is supported by the recent study showing that transcript levels of *LCIA* and *HLA3* were simultaneously impaired in an HC-requiring mutant containing a disrupted *CAS* gene encoding a putative chloroplast calcium sensor protein and that other LC-inducible genes, such as *CAH1*, *LCI1*, *LCIB*, and *LCIC*, were unaffected in the *CAS* mutant (34). Furthermore, this suggested that LCIA and HLA3 could function cooperatively as part of the CCM and that LCIA has a key role in guaranteeing the maintenance of the HCO_3^- uptake system. Because LCIA and HLA3 are conserved among aquatic algae, and owing to the structural relationship of LCIA homologs with aquaporin (33), the *LCIA* and *HLA3* genes may have potential for genetic improvement of photosynthesis in land plants and algae.

Materials and Methods

C. reinhardtii strain C9 (photosynthetically WT strain available from the National Institute for Environmental Studies, Japan, as strain NIES-2235) was cultured in Tris-acetate-phosphate (TAP) medium for maintenance. For physiological experiments, cells were grown in liquid TAP medium for precultivation and diluted with modified high-salt medium [HSM (NH_4^+)] containing 9.35 mM NH_4Cl supplemented with 20 mM Mops (pH 7.0) to an OD_{730} of ~0.05 for photoautotrophic growth. To induce the expression of exogenous genes, cells grown in HSM (NH_4^+) medium for ~24 h to an OD_{730} of ~0.3 were collected by centrifugation and resuspended in fresh HSM (NO_3^-) containing 9.35 mM KNO_3 aerated with air enriched with 5% CO_2 (HC) or ordinary air containing 0.04% CO_2 (VLC). The culture conditions with combinations of medium and CO_2 concentrations are described as HC-NH_4^+, HC-NO_3^-, VLC-NH_4^+, and VLC-NO_3^-. For all culture conditions, cells were cultured at 25 °C with illumination at 80 μmol photons·m^{-2}·s^{-1}.

Additional experimental procedures and methods are listed in the *SI Materials and Methods*.

1. Cordat E, Casey JR (2009) Bicarbonate transport in cell physiology and disease. *Biochem J* 417(2):423–439.
2. Price GD, Badger MR, Woodger FJ, Long BM (2008) Advances in understanding the cyanobacterial CO2-concentrating-mechanism (CCM): Functional components, Ci transporters, diversity, genetic regulation and prospects for engineering into plants. *J Exp Bot* 59(7):1441–1461.
3. Uehlein N, Lovisolo C, Siefritz F, Kaldenhoff R (2003) The tobacco aquaporin NtAQP1 is a membrane CO2 pore with physiological functions. *Nature* 425(6959):734–737.
4. Nakajima K, Tanaka A, Matsuda Y (2013) SLC4 family transporters in a marine diatom directly pump bicarbonate from seawater. *Proc Natl Acad Sci USA* 110(5):1767–1772.
5. Jones HG (1992) *Plants and Microclimate: A Quantitative Approach to Environmental Plant Physiology* (Cambridge Univ Press, Cambridge, UK), 2nd Ed.
6. Badger MR, Price GD (2003) CO2 concentrating mechanisms in cyanobacteria: Molecular components, their diversity and evolution. *J Exp Bot* 54(383):609–622.
7. Giordano M, Beardall J, Raven JA (2005) CO2 concentrating mechanisms in algae: Mechanisms, environmental modulation, and evolution. *Annu Rev Plant Biol* 56:99–131.
8. Badger MR, Kaplan A, Berry JA (1980) Internal inorganic carbon pool of *Chlamydomonas reinhardtii*: Evidence for a carbon-dioxide concentrating mechanism. *Plant Physiol* 66(3):407–413.
9. Moroney JV, Ynalvez RA (2007) Proposed carbon dioxide concentrating mechanism in *Chlamydomonas reinhardtii*. *Eukaryot Cell* 6(8):1251–1259.
10. Spalding MH (2008) Microalgal carbon-dioxide-concentrating mechanisms: *Chlamydomonas* inorganic carbon transporters. *J Exp Bot* 59(7):1463–1473.
11. Moroney JV, et al. (2011) The carbonic anhydrase isoforms of *Chlamydomonas reinhardtii*: Intracellular location, expression, and physiological roles. *Photosynth Res* 109(1-3):133–149.
12. Ohad I, Siekevitz P, Palade GE (1967) Biogenesis of chloroplast membranes. I. Plastid dedifferentiation in a dark-grown algal mutant (*Chlamydomonas reinhardi*). *J Cell Biol* 35(3):521–552.
13. Karlsson J, et al. (1998) A novel alpha-type carbonic anhydrase associated with the thylakoid membrane in *Chlamydomonas reinhardtii* is required for growth at ambient CO2. *EMBO J* 17(5):1208–1216.
14. Raven JA (1997) Putting the C in phycology. *Eur J Phycol* 32(4):319–333.
15. Vance P, Spalding MH (2005) Growth, photosynthesis, and gene expression in *Chlamydomonas* over a range of CO2 concentrations and CO2/O2 ratios: CO2 regulates multiple acclimation states. *Can J Bot* 83(7):796–809.
16. Wang Y, Spalding MH (2014) Acclimation to very low CO2: Contribution of limiting CO2 inducible proteins, LCIB and LCIA, to inorganic carbon uptake in *Chlamydomonas reinhardtii*. *Plant Physiol* 166(4):2040–2050.
17. Fukuzawa H, et al. (2001) Ccm1, a regulatory gene controlling the induction of a carbon-concentrating mechanism in *Chlamydomonas reinhardtii* by sensing CO2 availability. *Proc Natl Acad Sci USA* 98(9):5347–5352.
18. Xiang Y, Zhang J, Weeks DP (2001) The *Cia5* gene controls formation of the carbon concentrating mechanism in *Chlamydomonas reinhardtii*. *Proc Natl Acad Sci USA* 98(9):5341–5346.
19. Miura K, et al. (2004) Expression profiling-based identification of CO2-responsive genes regulated by CCM1 controlling a carbon-concentrating mechanism in *Chlamydomonas reinhardtii*. *Plant Physiol* 135(3):1595–1607.
20. Yamano T, Miura K, Fukuzawa H (2008) Expression analysis of genes associated with the induction of the carbon-concentrating mechanism in *Chlamydomonas reinhardtii*. *Plant Physiol* 147(1):340–354.
21. Brueggeman AJ, et al. (2012) Activation of the carbon concentrating mechanism by CO2 deprivation coincides with massive transcriptional restructuring in *Chlamydomonas reinhardtii*. *Plant Cell* 24(5):1860–1875.
22. Fang W, et al. (2012) Transcriptome-wide changes in *Chlamydomonas reinhardtii* gene expression regulated by carbon dioxide and the CO2-concentrating mechanism regulator CIA5/CCM1. *Plant Cell* 24(5):1876–1893.
23. Burow MD, Chen ZY, Mouton TM, Moroney JV (1996) Isolation of cDNA clones of genes induced upon transfer of *Chlamydomonas reinhardtii* cells to low CO2. *Plant Mol Biol* 31(2):443–448.
24. Im CS, Grossman AR (2002) Identification and regulation of high light-induced genes in *Chlamydomonas reinhardtii*. *Plant J* 30(3):301–313.
25. Ohnishi N, et al. (2010) Expression of a low CO2-inducible protein, LCI1, increases inorganic carbon uptake in the green alga Chlamydomonas reinhardtii. *Plant Cell* 22(9):3105–3117.
26. Yoshioka S, et al. (2004) The novel Myb transcription factor LCR1 regulates the CO2-responsive gene *Cah1*, encoding a periplasmic carbonic anhydrase in *Chlamydomonas reinhardtii*. *Plant Cell* 16(6):1466–1477.
27. Mariscal V, et al. (2006) Differential regulation of the *Chlamydomonas Nar1* gene family by carbon and nitrogen. *Protist* 157(4):421–433.
28. Duanmu D, Miller AR, Horken KM, Weeks DP, Spalding MH (2009) Knockdown of limiting-CO2-induced gene *HLA3* decreases HCO_3^- transport and photosynthetic Ci affinity in *Chlamydomonas reinhardtii*. *Proc Natl Acad Sci USA* 106(14):5990–5995.
29. Norling B, Nurani G, Franzen LG (1996) Characterization of the H⁺-ATPase in plasma membranes isolated from the green alga *Chlamydomonas reinhardtii*. *Physiol Plant* 97(3):445–453.
30. Ramazanov Z, Mason CB, Geraghty AM, Spalding MH, Moroney JV (1993) The low CO2-inducible 36-kilodalton protein is localized to the chloroplast envelope of *Chlamydomonas reinhardtii*. *Plant Physiol* 101(4):1195–1199.
31. Gonzalez-Ballester D, et al. (2011) Reverse genetics in *Chlamydomonas*: A platform for isolating insertional mutants. *Plant Methods* 7:24.
32. Yamano T, et al. (2010) Light and low-CO2-dependent LCIB-LCIC complex localization in the chloroplast supports the carbon-concentrating mechanism in *Chlamydomonas reinhardtii*. *Plant Cell Physiol* 51(9):1453–1468.
33. Wang Y, et al. (2009) Structure of the formate transporter FocA reveals a pentameric aquaporin-like channel. *Nature* 462(7272):467–472.
34. Wang L, Yamano T, Kajikawa M, Hirono M, Fukuzawa H (2014) Isolation and characterization of novel high-CO2-requiring mutants of *Chlamydomonas reinhardtii*. *Photosynth Res* 121(2-3):175–184.